Biochimica et Biophysica Acta, 1147 (1993) 50–58

BBAMEM 75938

Self-assembling properties of synthetic peptidic lipids

Toshimi Shimizu and Masakatsu Hato

Surface Engineering Laboratory, Research Institute for Polymers and Textiles, Tsukuba, Ibaraki (Japan)

(Received 12 October 1992)

Key words: Critical aggregate concentration (CAC); Morphology; Peptidic lipid; Self assembling; DSC

Novel peptidic lipids were synthesized by the coupling of a linear oligopeptide as the hydrophilic moiety with a glutamic acid dialkylamide as the hydrophobic moiety. Their self-assembling properties were investigated. The critical aggregate concentrations (CAC) for the peptidic lipids with a double dodecyl group were in the range of $1.0 \cdot 10^{-5}$–$3.8 \cdot 10^{-5}$ M. The phase transition parameters and the aggregation morphologies in aqueous dispersion were largely dependent on the number and nature of the constitutive amino acid residues. Dark-field optical microscopy demonstrated that the present peptidic lipids can form four types of stable morphologies in water, i.e., tubular structures, twisted ribbons, vesicles, and amorphous crystals.

Introduction

Peptides generally assume a specific conformation that helps to determine their physicochemical activity. Some proteins can self-assemble to function as flagella, tobacco mosaic virus, ribosomes, etc. In every case, spatial arrangements of the peptide chains play an important role in forming such molecular assemblies. In globular proteins, six levels of structural organization can be distinguished [1]. Among them, primary and secondary structures of proteins so far have been mimicked by using synthetic homo-poly(amino acid)s [2,3]. However, it is too difficult to predict higher levels of ordered structures for synthetic peptides, because they are stabilized by a complex network of complementary intra- and interchain forces. In our previous study, we observed an enhanced circular dichroism (CD) by peptidic lipids in the 200–250 nm region [4]. This phenomenon supports the existence of regular inter- and intramolecular arrangements of the amide-bond chromophore in the assembly. Thus, we turned our attention to the physicochemical understanding of the self-assembling behavior exhibited by such peptidic lipids.

A great number of studies on self-assembling properties of phospholipids have been carried out to determine the structure and energetics of the biomembrane [5–7]. Extensive studies on synthetic bilayer-forming compounds have also greatly contributed to the understanding of biomembrane behavior [8–11]. Recently, synthetic lipids bearing an oligosaccharide [12,13], a poly(amino acid) [14], or a nucleotide [15] as the hydrophilic moiety, have been prepared to investigate the headgroup function in the formation of specific aggregation morphologies. As a result, it has been found that specific morphologies such as a helix can be formed by the intermolecular hydrogen bonding and the stereoselective interaction between chiral headgroups [16].

In this paper, we wish to report the approach of arranging peptide moieties by self-assembly and the formation of special superstructures. This approach utilizes synthetic peptidic lipids that consist of a linear oligopeptide as the hydrophilic region and a glutamate-derived double hydrocarbon chain as the hydrophobic region. We describe the synthesis of peptidic lipids (**1**–**8**) shown in Table I and their self-assembling properties in aqueous dispersions. In the present study, we have synthesized four amino acid trimers (**1**, **2**, **3**, and **7**) and two amino acid tetramers (**4** and **8**), which contain glycine, sarcosine, or proline residues as the hydrophilic peptidic moiety. In addition, we have also adopted the amino acid sequence of Gly-Lys(Z)-Sar-Pro in **5** and Gly-Lys-Sar-Pro in **6** as a related segment to the synthetic peptidic Ca^{2+}-ionophore [17,18]. The

Correspondence to: T. Shimizu, Surface Engineering Laboratory, Research Institute for Polymers and Textiles, 1-1-4 Higashi, Tsukuba, Ibaraki 305, Japan.

Abbreviations: Boc, *t*-butoxycarbonyl; CD, circular dichroism; DEPC, diethyl phosphorocyanidate; DPPA, diphenylphosphoryl azide; DMF, dimethylformamide; DSC, differential scanning calorimetry; m.p., melting point; -NHC12, dodecylamino; -NHC18, octadecylamino; OSu, *N*-hydroxysuccinimide ester; TEA, triethylamine; TFA, trifluoroacetic acid; Z, carbobenzoxy.

TABLE I

Constitutive amino acid residues in the peptidic lipids that we have synthesized

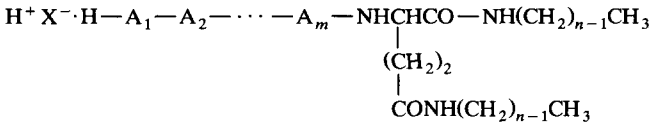

Peptidic lipid	X	A_1	A_2	A_3	A_4	*m*	*n*
1	Cl	Gly	Gly	Gly	–	3	12
2	Cl	Sar	Sar	Sar	–	3	12
3	Cl	L-Pro	L-Pro	L-Pro	–	3	12
4	Cl	L-Pro	L-Pro	L-Pro	L-Pro	4	12
5	Cl	Gly	L-Lys(Z)	Sar	L-Pro	4	12
6	Br	Gly	L-Lys	Sar	L-Pro	4	12
7	Cl	Sar	Sar	Sar	–	3	18
8	Cl	Sar	Sar	Sar	Sar	4	18

physical parameters used for characterization of the amino-acid effects are critical aggregate concentrations (CAC), thermodynamic transition parameters by differential scanning calorimetry (DSC), and morphology assignments by dark-field optical microscopy.

Materials and Methods

Synthesis of peptidic lipids

Peptidic lipids were synthesized according to the following route. The peptide chain of the hydrophilic region was elongated through the N-terminal. The conventional procedure of peptide synthesis gave the linear oligopeptides, Boc-Gly-Gly-Gly-OH (a white solid, m.p. 125–127°C), Boc-Sar-Sar-Sar-OH (a white semisolid), Boc-Sar-Sar-Sar-Sar-OH (a white semisolid), Boc-Pro-Pro-Pro-OH (a white solid, m.p. 189–191°C), Boc-Pro-Pro-Pro-Pro-OH (a white solid, m.p. 95–98°C), and Boc-Gly-Lys(Z)-Sar-Pro-OH (a white solid, m.p. 78–80°C). Glutamic acid dialkylamide derivatives, HBr · H-L-Glu[$NH(CH_2)_{11}CH_3$]-$NH(CH_2)_{11}CH_3$ (hereafter abbreviated as HBr · H-Glu(NHC12)-NHC12) and HBr · H-L-Glu[$NH(CH_2)_{17}CH_3$]-$NH(CH_2)_{17}CH_3$ (hereafter abbreviated as HBr · H-Glu(NHC18)-NHC18) were obtained by the coupling of carbobenzoxy-L-glutamic acid α, γ-di-*N*-hydroxysuccinimide ester [Z-Glu(OSu)-OSu] with dodecylamine and octadecylamine, respectively. Finally, condensation between the peptide moiety and the glutamic acid derivative was accomplished by the use of diphenylphosphoryl azide (DPPA) or diethyl phosphorocyanidate (DEPC) as a coupling reagent. DEPC was much more reactive than DPPA. Treating the product with hydrogen halide produced the hydrogen halide salt, which has amphiphilic character. All synthetic intermediates were purified by medium-pressure liquid chromatography with silica-gel (Merck Lichroprep Si 60). The purity of each compound was confirmed by elemental analysis, thin-layer chromatography, and 67.5 MHz ^{13}C-NMR spectroscopy.

HBr · H-Glu(NHC12)-NHC12. A solution of Z-Glu(OSu)-OSu (1.00 g, 2.10 mmol) and dodecylamine (0.78 g, 4.21 mmol) in chloroform (20 ml) was allowed to stand at room temperature for 2 days. The chloroform solution was washed with an aqueous 4% sodium bicarbonate solution and then water before drying over anhydrous sodium sulfate. Evaporation of chloroform left a white solid of Z-Glu(NHC12)-NHC12; yield, 1.17 g (91%); m.p., 138–139°C.

A solution of this compound (0.83 g, 1.35 mmol) in trifluoroacetic acid (TFA) (3 ml) was treated with 25% HBr/acetic acid (4.2 ml) at room temperature for 2 h. The precipitate was filtered and taken up in ether. An oily residue obtained by evaporation of ether was solidified from a water/methanol/chloroform mixture; yield, 0.74 g (98%); m.p., 118–122°C. Anal.: Calcd. for $C_{29}H_{60}O_2N_3Br$: C, 61.90; H, 10.75; N, 7.47. Found: C, 61.57; H, 10.69; N, 7.61.

HBr · H-Glu(NHC18)-NHC18 was obtained in the same manner as mentioned above; yield, 1.28 g (92%); m.p. 125–127°C. Anal.: Calcd. for $C_{41}H_{84}O_2N_3Br$: C, 67.36; H, 11.58; N, 5.75. Found: C, 66.97; H, 11.12;, N, 5.91.

HCl · H-Gly-Gly-Gly-Glu(NHC12)-NHC12 (1) and HCl · H-Pro-Pro-Pro-Glu(NHC12)-NHC12 (3). These peptidic lipids were synthesized as reported elsewhere [19].

HCl · H-Sar-Sar-Sar-Glu(NHC12)-NHC12 (2). A solution of DEPC (0.45 g, 2.76 mmol) in dimethylformamide (DMF) (2 ml) was added to a solution of Boc-Sar-Sar-Sar-OH (0.77 g, 2.32 mmol) and HBr · H-Glu(NHC12)-NHC12 (1.57 g, 2.79 mmol) at 0°C with stirring, followed by the addition of a solution of triethylamine (TEA) (0.72 ml, 5.14 mmol) in DMF (2 ml). Stirring was continued at 0°C for 6 h and at room temperature overnight. The reaction mixture was diluted with chloroform (100 ml) and washed with 10% citric acid (50 ml × 2), 4% sodium bicarbonate (50 ml × 2), saturated aqueous sodium chloride aqueous solution (50 ml × 2) and distilled water (50 ml × 2). The chloroform layer was dried over anhydrous sodium sulfate. Evaporation of the solvent left Boc-Sar-Sar-Sar-Glu(NHC12)-NHC12 as a white gel. Drying under reduced pressure gave a white solid; yield, 2.00 g (100%). This product (1.84 g, 2.31 mmol) was dispersed in ethyl acetate (10 ml) and treated with 4 M HCl/ethyl acetate (17 ml) at room temperature for 1 h. Evaporation of the solvent gave a white solid. Recrystallization from a water/methanol/chloroform mixture gave **2** as a white solid; yield, 260 mg (15%).

HCl · H-Pro-Pro-Pro-Pro-Glu(NHC12)-NHC12 (4). A solution of DPPA (0.27 ml, 1.24 mmol) in DMF (5 ml) was added to a solution of Boc-Pro-Pro-Pro-Pro-OH

(II) (0.53 g, 1.04 mmol) and HBr · H-Glu(NHC12)-NHC12 (0.70 g, 1.24 mmol) in DMF (50 ml) at 0°C with stirring, followed by the addition of a solution of TEA (0.32 ml, 2.29 mmol) in DMF. By the same treatment as described for **2**, Boc-Pro-Pro-Pro-Pro-Glu(NHC12)-NHC12 was obtained as a white solid. The product was purified by silica-gel column chromatography (chloroform/methanol (5 : 1, v/v)). A pale yellow oil (0.65 g) was dissolved in ethyl acetate (10 ml) and treated with 3.5 N HCl/ethyl acetate (10 ml) at room temperature for 1 h. Evaporation of the solvent left a pale yellow oil. Recrystallization from a water/methanol/chloroform mixture gave **4** as a white solid; yield, 400 mg (77%).

HCl · H-Gly-Lys(Z)-Sar-Pro-Glu(NHC12)-NHC12 (5). Boc-Gly-Lys(Z)-Sar-Pro-OH (1.00 g, 1.65 mmol) and HBr · H-Glu(NHC12)-NHC12 (1.11 g, 1.98 mmol) was coupled by DEPC (0.34 g, 2.08 mmol) and TEA (0.51 ml, 3.64 mmol) in the same manner as described for **2**. In this way, Boc-Gly-Lys(Z)-Sar-Pro-Glu-(NHC12)-NHC12 was obtained as a white solid; yield, 1.50 g (85%); m.p., 71–73°C. This product (0.29 g, 0.27 mmol) was dissolved in chloroform (6 ml) and treated with 4 M HCl/ethyl acetate in the same manner as described for **4**. A colorless syrup obtained was crystallized from water. Lyophilization of the colloidal aqueous solution left a pure white solid; yield, 270 mg (99%).

2HBr · H-Gly-Lys-Sar-Pro-Glu(NHC12)-NHC12 (6). Boc-Gly-Lys(Z)-Sar-Pro-Glu(NHC12)-NHC12 (0.70 g, 0.66 mmol) was dissolved in ethyl acetate (6 ml) and treated with 25% HBr/acetic acid (56 ml, 13 mmol) at room temperature for 2 h. Evaporation of the solvent gave a pale yellow oil, to which a small amount of water (10 ml) was added. Lyophilization of the colloidal solution left a pale yellow solid; yield, 600 mg (92%).

HCl · H-Sar-Sar-Sar-Glu(NHC18)-NHC18 (7). Boc-Sar-Sar-Sar-OH (0.30 g, 0.91 mmol) and HBr · H-Glu(NHC18)-NHC18 (0.79 g, 1.09 mmol) was coupled by DEPC (0.18 g, 1.09 mmol) and TEA (0.28 ml, 1.99 mmol), and the product was debutoxycarbonylated with 4 N HCl/ethyl acetate in the same manner as described for **2**. In the course of the synthesis, Boc-Sar-Sar-Sar-Glu(NHC18)-NHC18 was purified by silica-gel column chromatography (chloroform/methanol (5 : 1, v/v)); yield, 230 mg (95%).

HCl · H-Sar-Sar-Sar-Sar-Glu(NHC18)-NHC18 (8). Boc-Sar-Sar-Sar-Sar-OH (0.40 g, 0.99 mmol) and HBr · H-Glu(NHC18)-NHC18 (0.87 g, 1.19 mmol) was coupled by DEPC (0.19 g, 1.19 mmol) and TEA (0.31 ml, 2.19 mmol), and the product was debutoxycarbonylated with 4 M HCl/ethyl acetate in the same manner as described for **2**. All products were purified by silica-gel column chromatography (chloroform/methanol (5 : 1, v/v)); yield, 260 mg (68%).

Observation of morphologies of aggregates in aqueous dispersions

1 ml of deionized double-distilled water was added to 1 mg of peptidic lipid. The aqueous dispersion was sonicated at a temperature about 10°C higher than the corresponding phase transition temperature. The pH range of the obtained aqueous media was 5.9–6.5 for all peptidic lipids (**1–8**). Therefore, the amino groups of the lipids should be in the protonated state. The sonicated dispersion was then allowed to stand at room temperature (23–25°C) for a specified time. A drop of the dispersion was placed on the slide glass, covered with a coverslip, and sealed at the edges with adhesive tape. Samples were examined by dark-field optical microscopy [20] (Olympus BHS, 200-W Xe lamp, magnification 900–1500 ×).

General measurement

For differential scanning calorimetry (DSC), weighed quantities of peptidic lipids (1–2 mg) were dispersed in 50 μl of deionized double-distilled water by sonication. The same thermodynamic data were also obtained when buffered solutions (pH 5.0–6.0) were used in-

TABLE II

Analytical data of peptidic lipids

Peptidic lipid	Formula	Elemental analysis [a] (%)			m.p. (°C)	$[\alpha]_D^{22}$
		C	H	N		
1	$C_{35}H_{69}O_5N_6Cl \cdot (3/2)H_2O$	58.88 (58.67)	9.76 (10.12)	11.18 (11.73)	208–209	n.d. [b]
2	$C_{38}H_{75}O_5N_6Cl \cdot (1/2)H_2O$	61.45 (61.63)	10.38 (10.34)	11.12 (11.35)	163–164	−7.85 (c = 1.07, ethanol)
3	$C_{44}H_{81}O_5N_6Cl \cdot H_2O$	63.61 (63.86)	9.95 (10.11)	10.03 (10.15)	89– 91	−81.26 (c = 1.05, ethanol)
4	$C_{49}H_{88}O_6N_7Cl \cdot (5/2)CH_3OH$	63.02 (62.68)	9.94 (10.00)	9.42 (9.93)	76– 78	−81.58 (c = 1.07, ethanol)
5	$C_{53}H_{93}O_8N_8Cl \cdot (5/2)H_2O$	60.87 (60.58)	9.17 (9.40)	10.21 (10.66)	107–110	−35.42 (c = 1.05, ethanol)
6	$C_{45}H_{88}O_6N_8Br_2 \cdot HBr \cdot 5H_2O$	46.30 (46.27)	8.36 (8.54)	8.98 (9.59)	189–195	−29.73 (c = 1.15, ethanol)
7	$C_{50}H_{99}O_5N_6Cl \cdot (5/2)H_2O$	63.24 (63.56)	10.98 (11.09)	8.63 (8.89)	175–178	−4.93 (c = 0.16, chloroform)
8	$C_{53}H_{104}O_6N_7Cl \cdot (3/2)CH_3OH$	64.76 (64.24)	10.64 (10.88)	9.03 (9.62)	130–135	−4.08 (c = 0.27, chloroform)

[a] Calculated values are given in parentheses.

[b] Not determined since **1** was practically insoluble in common organic solvents.

stead of deionized double-distilled water. All measurements were run on a Seiko Denshi SSC 560U calorimeter at a scanning rate of 1.0°C/min. The surface tension was measured by the Wilhelmy method with a Kyowa Kaimen Kagaku CBVP-A3 surface-tension apparatus in a class 100 clean room. For the measurement, a peptidic lipid was dissolved in chloroform to prepare a 10 mM mother liquor. An accurately known volume of the peptide solution was placed in the vial. After drying in vacuo, aqueous solutions (10^{-6}–10^{-3} M) were prepared by adding deionized double-distilled water and then sonicating. These solutions were allowed to stand for more than 1 day at room temperature.

Results and Discussion

General properties

The analytical data for the peptidic lipids are summarized in Table II. Hopp et al. [21] have provided a set of values expressing the relative hydrophilicity of each amino acid. According to this information, the relative hydrophilicity values of the lysine, glycine, and proline residues are estimated to be 3.0, 0.0, and 0.0, respectively. It is safe to assume that the sarcosine residue (although the data are not shown) has a value similar to that of the proline and glycine residues. Therefore, except for lysine, the amino acid residues utilized in this study, i.e., glycine, sarcosine, and proline, are intermediate between the hydrophobic residues and hydrophilic residues. Double-chain alkyl derivatives with poly(L-glutamic acid)- [14] or poly(L-aspartic acid) headgroups [22] have been synthesized by Yamada et al. and Ihara et al., respectively. However, those compounds are a mixture of amphiphiles with a certain degree of polymerization. Besides the lysine residue, the amino acids employed by us are not charged or polar residues like glutamic acid and aspartic acid. Furthermore, our amphiphiles are regarded as a peptide which consists of only an α-amino acid component. From these viewpoints, the present peptidic lipids are substantially different from peptide-containing amphiphiles [14,22,23–25].

Another important characteristic of sarcosine and proline is that they allow the introduction of *N*-substituted amino acid residues into the hydrophilic headgroup. These residues have no ability to act as hydrogen-bonding donors because of the lack of amide NH protons. Actually, the peptidic lipid **1**, which has three glycine residues, gave a white amorphous precipitate when it was sonicated in water at 70–80°C for 10–20 min. This poor dispersibility into water probably originates from strong intermolecular hydrogen bondings between glycine residues. On the other hand, good turbid aqueous dispersions were obtained by the addition of water and gentle shaking at room temperature with the peptidic lipids (**2–6**). The peptidic lipids **7** and **8** with a double octadecylamino group gave a turbid dispersion only after sufficient sonication at 80–90°C.

TABLE III

Critical aggregate concentration (CAC) of peptidic lipids

Peptidic lipid or amphiphile	CAC (M)	Ref.
2	$3.8 \cdot 10^{-5}$	
3	$1.2 \cdot 10^{-5}$	
4	$3.1 \cdot 10^{-5}$	
6	$1.0 \cdot 10^{-5}$	
$(CH_3)_3N^+(CH_2)_{11}CH_3Br^-$	$1.5 \cdot 10^{-2}$	[27]
$(CH_3)_3N^+(CH_2)_5CH_3Br^-$	$9.2 \cdot 10^{-4}$	[27]
$CH_3(CH_2)_{11}OSO_3Na$	$8.1 \cdot 10^{-3}$	[27]
1,2-Didecanoyl-*sn*-glycero-3-phosphocholine	$5 \cdot 10^{-6}$	[28]
1,2-Dipalmitoyl-*sn*-glycero-3-phosphocholine	$< 10^{-10}$	[29]

Critical aggregate concentration (CAC)

The critical aggregate concentrations were determined from the break points of plots of lipid concentration vs. surface tension. The CAC values obtained for the four peptidic lipids (**2**, **3**, **4**, and **6**) are summarized in Table III. The CAC values are in the range of $1.0 \cdot 10^{-5}$–$3.8 \cdot 10^{-5}$ M. They are not significantly affected by the structural characteristics of the amino acid residues when the length of hydrocarbon chain is fixed. The values agree with those of quarternary ammonium salts containing amino acid residues ($3 \cdot 10^{-6}$–$2 \cdot 10^{-5}$ M) [23] and those of synthetic ammonium amphiphiles bearing the same length of double hydrocarbon chain ($8 \cdot 10^{-6}$–$3 \cdot 10^{-5}$ M) [26]. These amphiphiles are well known to form bilayer assemblies in dilute aqueous solution [23,26]. For comparison, CAC values of representative surfactants and naturally occurring phospholipids are also available [27–29]. Micelle-forming compounds bearing a single long hydrocarbon chain have higher CAC values ($> 9.2 \cdot 10^{-4}$ M) than those of the peptidic lipids, while phosphatidylcholine-derivatives forming liposomes have much lower CAC values ($< 10^{-6}$ M).

Differential scanning calorimetry (DSC)

In order to gain information about the phase transition of the peptide assembly, we performed thermodynamic measurements with a differential scanning calorimeter. Each aqueous dispersion of the peptidic lipid (1–5 wt%) gave one endothermic peak at 23–103°C on heating, which may be safely ascribed to a gel/liquid-crystal phase transition. This feature could be confirmed by polarizing optical microscopy. At temperatures above the DSC-determined phase transition, a focal conic texture could be observed between crossed nicol prisms, suggesting the existence of lamellar struc-

TABLE IV

Phase transition parameters for peptidic lipids in aqueous dispersions

Amphiphile	Concentration (w/w, %)	T_m (°C)	ΔH (kJ/mol)
1	4.78	103	n.d. [a]
2	1.22	47	35.6
3	1.89	31	7.3
4	2.06	22	3.5
5	1.84	53	28.0
6	1.60	39	23.4
7	1.80	80	62.8
8	1.94	79	51.9

[a] Not determined.

ture [30]. The phase transition temperature (T_m) and the enthalpy change (ΔH) were evaluated from the endothermic peak minimum and the peak area, respectively, and they are summarized in Table IV.

When peptidic lipids having both identical alkyl-chain length and the same number of residues are compared (**1**, **2**, and **3**), the trisarcosine-containing lipid **2** exhibits a phase transition temperature higher than that of the triproline-containing lipid **3**, but considerably lower than that of the triglycine-containing lipid **1**. The number of constituent amino acid residues also affects the phase transition behavior of the aqueous dispersion. The introduction of one proline residue to the triproline derivative **3** lowers the T_m value from 31 to 22°C when the alkyl chain length is fixed as a dodecyl group (**3** and **4**). This contribution, however, cannot be notably observed for the sarcosine derivatives with a double octadecyl group (**7** and **8**). The replacement of a hydrophobic ϵ-carbobenzoxy-lysine residue (Lys(Z)) with a cationic lysine residue (Lys) also lowers the T_m value from 53 to 39°C (**5** and **6**). The T_m value of the peptidic lipid **7** with a double octadecyl group is larger than that of **2** with a double dodecyl group (5.5°C change per methylene group). As predicted from the literature [31,32], increasing alkyl chain length shifts the endothermic peak to higher temperatures, provided the number of residues is fixed.

Since the internal rotation around the proline N-C^{α} bond is restricted, oligoproline tends to maintain a well-defined and rigid conformation. The CD spectra of the tri- and tetraproline-containing lipids (**3** and **4**) in aqueous solution suggested that they exist in a left-handed helical conformation with a *trans* peptide bond in the assembly [2,33–34] (Fig. 1c). Accordingly, the 3-dimensional arrangement of the tri- or tetraproline moiety will keep the headgroup volume of these lipids larger in comparison to the other peptidic lipids. Actually, monolayer studies demonstrated that the limiting molecular area of the tetraproline-containing lipid **4** is about 2-times larger (~ 100 Å^2) than that of the sarcosine- or glycine-containing lipids (unpublished data). Thus, the backbone of the trisarcosine and the triglycine can be assumed to take an extended form with a *trans* peptide bond (Fig. 1a, b). From the findings discussed above, the bulkiness of the triproline headgroup would perturb the effective hydrophobic interaction between alkyl chains, compared to the trisarcosine derivatives. Relatively lower values of both T_m and ΔH for the proline-containing lipids **3** and **4** are closely related to these features. In contrast, the property of glycine residues to impart higher stability (T_m) is probably ascribed to the lower degree of hydration. Such a situation promotes the hydrogen-bond formation between glycine moieties. On the other hand, sarcosine has an intermediate character between glycine and proline and is able to hydrogen bond to water molecules to some degree. Table IV shows that the T_m values are more sensitive to the nature of constitutive amino acid residues than the number of residues.

The dependence of ΔH on the alkyl chain length and the headgroup is apparently complex. The increase in the hydrocarbon chain length gives a larger ΔH value, assuming the hydrophilic groups are equivalent (**2** and **7**). However, an increase in the number of residues causes a decrease in ΔH (**3** and **4**) (**7** and **8**). This implies that the decrease in intermolecular forces between lipids is closely correlated to the headgroup size. The triproline-containing lipid **3** gave a relatively smaller ΔH, compared with the trisarcosine derivative **2**. Headgroup–headgroup interactions in the oligopro-

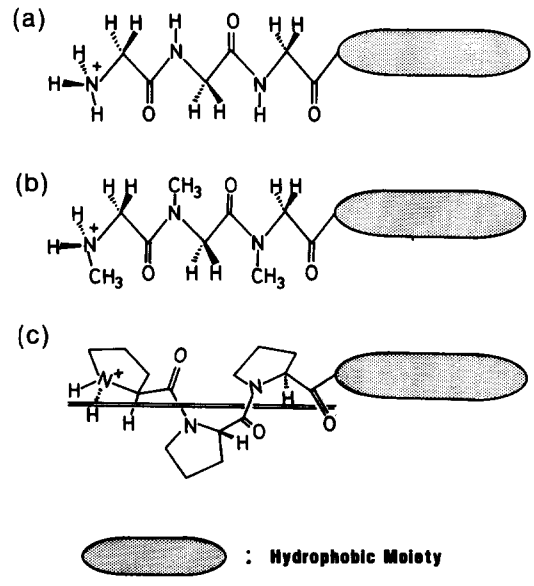

Fig. 1. Most possible conformations of the oligopeptide-head groups in peptidic lipids **1–3**. (a) a planar zig-zag conformation with a *trans* peptide bond proposed for HCl·H-Gly-Gly-Gly-Glu(NHC12)-NHC12 (**1**), (b) a similar conformation of HCl·H-Sar-Sar-Sar-Glu(NHC12)-NHC12 (**2**) as that proposed for **1**, and (c) a left-handed helical conformation with a *trans* peptide bond proposed for HCl·H-Pro-Pro-Pro-Glu(NHC12)-NHC12 (**3**).

line-containing lipids are presumably weaker than the hydrophobic interactions because of the steric bulkiness of the headgroups. The ΔH values also depend strongly on the length of the alkyl chain. In the case of sarcosine derivatives, the increase in ΔH is estimated to be 1.1 kcal/mol per methylene group.

Morphology of aggregate

Morphologies of the aggregates were observed by dark-field optical microscopy. This methodology is efficient, because the aggregate structure can be directly elucidated in the presence of water and monitored with time [20,35].

After the sonication of each aqueous dispersion at a temperature above the corresponding T_m, the morphological change of the aggregate was monitored at room temperature (23–25°C) for the peptidic lipids (**1**, **2**, **3**, **4**, **5**, and **6**) with a double dodecyl group. After 10–20 min of incubation time, very small particles ($\ll 1$ μm) were observed on the optical microscope for all peptidic lipids. However, the structure of the aggregate underwent a gradual change from a very small particle to another specific morphology over a period of hours or days.

As a result, four representative growth process could be observed, depending on the head-group character. The first is a tubular structure [14,36,37] demonstrated by **3**, **5**, and **6**. This tube was stable at room temperature and showed no morphological change over a period of 6 months. In the course of this growth process, long flexible helical ribbons could be also detected as an intermediate structure. The growth features of the tubular structure via helices are shown in Fig. 2. The bar-graphs indicate the respective variation in the length of the helical and tubular structure. The tubular structure appears so rigid and straight that it is shorter in length (< 30 μm) than the helices. Fig. 3 shows a characteristic photograph which provides the evidence of an intermediary microstructure in the formation of a tubular structure. It shows a tubular aggregate connected to a helical ribbon structure. This structure is quite different from fused double-duplex strands [14,15] or widened ribbons [36]. Such a junction occurs at several places within a helix. The schematic transition process is shown in Fig. 4. The helical ribbon structure is metastable, because its hydrocarbon surface is exposed to water. The complete transition from helical ribbons to tubular structures required between 1 day and a few weeks. In the previous study with the triproline-containing lipid **3**, we reported a remarkable reduction in the length of the helical assemblies, which was induced by Ba^{2+} [33]. This approach is worthy of mention in terms of leading to the artificial control of the dimensions of the helical bilayer assembly [38].

The second characteristic morphology is the twisted ribbon which is produced by **2** (Fig. 5). To the best of our knowledge, such clear twisted ribbons were first directly observed by dark-field optical microscopy.

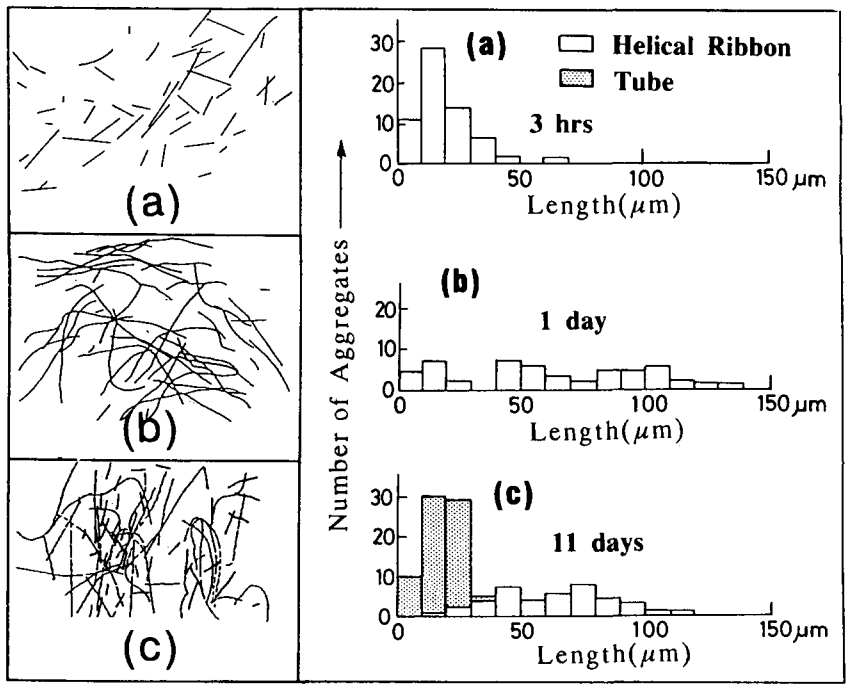

Fig. 2. Length distribution of helical ribbons and tubular structures formed by HCl·H-Pro-Pro-Pro-Glu(NHC12)-NHC12 (**3**). The length was directly measured from the optical micrograph. The concentration of the lipid was 1 mg/ml. The incubation times in aqueous dispersion were (a) 3 h, (b) 1 day, and (c) 11 days. Average length of the aggregate ($\bar{l}$) and the total number of measured aggregates (n) are (a) $\bar{l} = 19.4$ μm, $n = 51$, (b) $\bar{l} = 64.7$ μm, $n = 45$, and (c) $\bar{l} = 63.8$ μm, $n = 37$ for helical ribbons and $\bar{l} = 17.5$ μm, $n = 53$ for tubular structures.

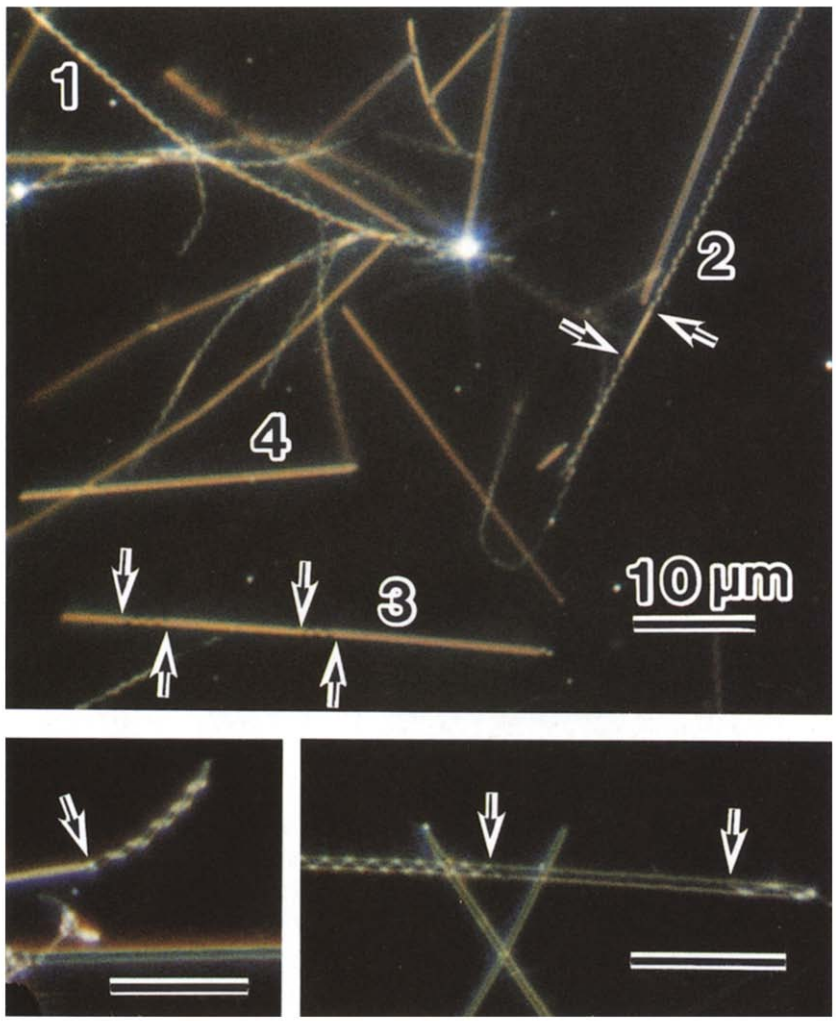

Fig. 3. Dark-field optical micrographs of aqueous dispersion of HCl·H-Pro-Pro-Pro-Glu(NHC12)-NHC12 (**3**, 1 mg/ml). The junction points where helical ribbon structures were connected to tubular structures, are denoted by arrows. The content of helical ribbon structure within a single aggregate decreases as we see from the helix (denoted as 1) to the tube (denoted as 4) in numerical order. The time of incubation is 1–3 days at room temperature. Magnification: scale bar, 10 μm.

Thickness of the ribbon was estimated to be 200–1000 Å from the lower limit of detection [20] and the width at the most constricted part (denoted by arrows in Fig. 5). Accordingly, the ribbons are composed of multiple bilayers. A similar microstructure has been also found in the aqueous dispersion of glucocerebroside from Gaucher's spleen [39]. Such a structure differs remarkably from the helically wound ribbon in the following respects. The center line of the ribbon is not helically wound, but almost straight or loosely curved. No twisted ribbons change into a tubular structure. As discussed above, the oligoproline derivatives **3** and **4** will take a left-handed helix (Fig. 1c) [2,33–34], because of the chirality of the proline residue and the restricted rotation around the N-C$^{\alpha}$ bond. Oligosarcosine has no chirality and will take an extended conformation. However, the trisarcosine-containing lipid **2** is a chiral compound owing to the existence of the glutamate residue. Therefore, the chirality of the amino acid residue and the head-group volume may be determinants in the formation of either a twisted ribbon or a helical ribbon. The growth mechanism of twisted ribbons will be distinct from that of helical ribbons. We detected that the width of the ribbon gradually increased without intertwisting and became prominent on the optical microphotograph. This means that a common crystal-

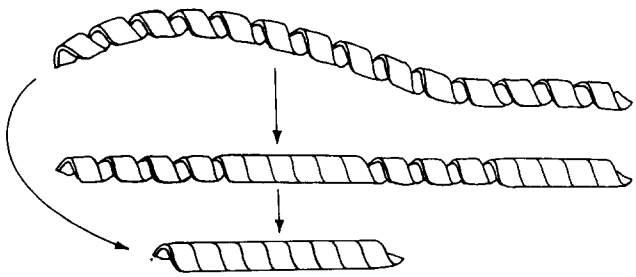

Fig. 4. Schematic illustration of the growth process for a helical ribbon structure to change into a tubular structure.

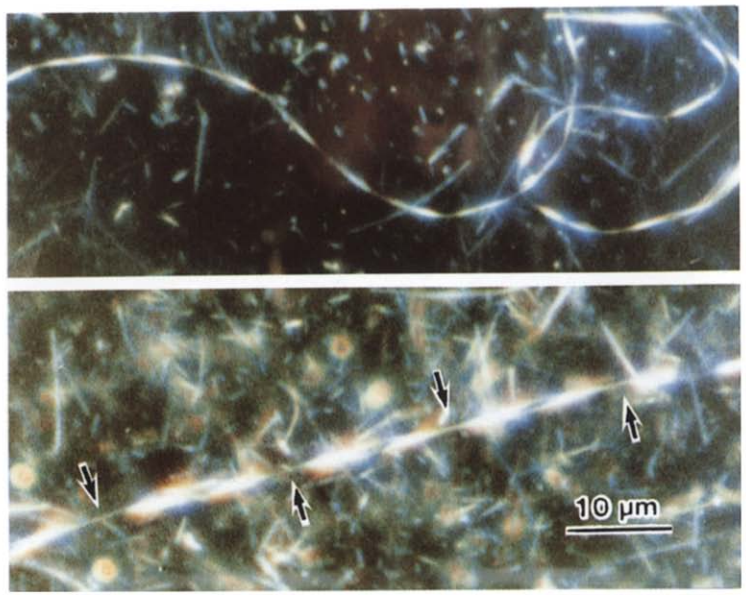

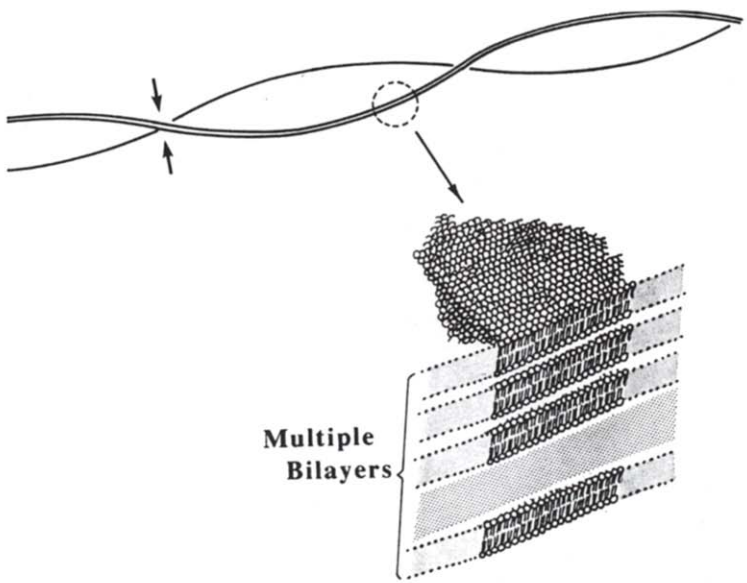

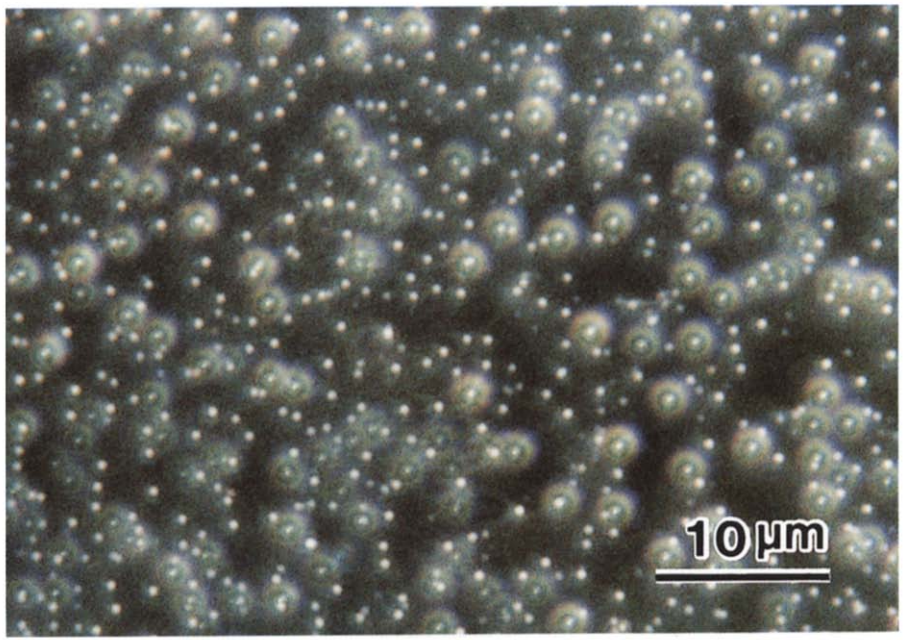

Fig. 6. Stable vesicles of HCl·H-Pro-Pro-Pro-Pro-Glu(NHC12)-NHC12 (**4**) obtained by dark-field optical microscopy. The time of incubation is 1 day at room temperature. Magnification: scale bar, 10 μm.

Fig. 5. Twisted ribbon structure of HCl·H-Sar-Sar-Sar-Glu(NHC12)-NHC12 (**2**) observed by dark-field optical microscopy. The time of incubation is 3 months at room temperature. The lower optical micrograph shows the most grown-up twisted ribbon structure (helical pitch: approx. 18 μm, width of ribbon: approx. 1.2 μm). Magnification: scale bar, 10 μm.

growth process is applicable as a growth mechanism for the self-assembling lipid **2**.

The third example is the formation of stable vesicles given by **4** (Fig. 6). All aggregation morphologies mentioned above were stable only at temperatures below each T_m. Upon heating them to a temperature above the T_m, they immediately converted from their characteristic morphology in the gel state into a vesicle form in the liquid-crystalline state. The hydrocarbon chains of **4** exist as a fluid state at room temperature, because the T_m of **4** is 22°C, so the tetraproline derivative **4** remains unchanged.

The final case is an amorphous crystal produced by **1**. This implies that favorable hydration is suppressed by the strong intermolecular hydrogen bonding between glycine residues.

In conclusion, novel peptidic lipids provided a number of aggregation morphologies in aqueous dispersion. The self-assembling properties of each peptidic lipid strongly depend on the number and nature of the constitutive amino acid residues.

References

1 Schulz, G.E. and Schirmer, R.H. (1979) in Principles of Protein Structure (Cantor, C.R., ed.), Chapter 5, Springer-Verlag, New York.
2 Beychok, S. (1967) in Poly-α-Amino Acids (Fasman, G.D., ed.), Marcel Dekker, New York.
3 Yang, J.T. (1967) in Poly-α-Amino Acids (Fasman, G.D., ed.), Marcel Dekker, New York.
4 Shimizu, T., Mori, M., Minamikawa, H. and Hato, M. (1989) Chem. Lett., 1341–1344.
5 Vance, E. (1984) in Biochemistry (Zubay, G., ed.), Addison-Wesley, Reading, MA.
6 Singer, S. and Nicholson, G.L. (1972) Science 175, 720–731.
7 Nojima, S., Sunamoto, J. and Inoue, K. (eds.) (1988) The Liposomes, Nankodo, Tokyo.
8 Kunitake, T. and Okahata, Y. (1977) J. Am. Chem. Soc. 99, 3860–3861.
9 Kunitake, T. (1979) J. Macromol. Sci. Chem. A13, 587–602.
10 Fendler, J. (ed.) (1982) Membrane Mimetic Chemistry, John Wiley and Sons, New York.
11 Ringsdorf, H., Schlarb, B. and Venzmer, J. (1988) Angew. Chem. Int. Edn. Engl. 27, 113–158.
12 Mannock, D.A., Lewis, R.N.A.H., Sen, A. and McElhaney, R.N. (1988) Biochemistry, 27, 6852–6859.
13 Hinz, H.-J., Kuttenreich, H., Meyer, R., Renner, M. and Fruend, R. (1991) Biochemistry 30, 5125–5138.
14 Yamada, K., Ihara H., Ide, T., Fukumoto, T. and Hirayama, C. (1984) Chem. Lett. 1713–1716.
15 Yanagawa, H., Ogawa, Y., Furuta, H. and Tsuno, K. (1989) J. Am. Chem. Soc. 111, 4567–4570.
16 Fuhrhop, J.-H. and Boettcher, C. (1990) J. Am. Chem. Soc. 112, 1768–1776.
17 Shimizu, T., Tanaka, Y. and Tsuda, K. (1985) Bull. Chem. Soc. Jpn. 58, 3436–3443.
18 Shimizu, T., Tanaka, Y. and Tsuda, K. (1986) Int. J. Pept. Protein Res. 27, 344–354.
19 Shimizu, T. and Hato, M. (1989) Thin Solid Films 180, 179–183.
20 Hotani, H. (1984) J. Mol. Biol. 178, 113–120.
21 Hopp, T.P. and Woods, K.R. (1981) Proc. Natl. Acad. Sci. USA 78, 3824–3828.
22 Ihara, H., Fukumoto, T., Hirayama, C. and Yamada, K. (1986) Polym. Commun. 27, 282–285.
23 Murakami, Y., Nakao, A. and Ikeda, H. (1982) J. Org. Chem. 47, 2137–2144.
24 Murakami, Y., Nakao, A., Yoshimatsu, A., Uchitomi, K. and Matsuda, Y. (1984) J. Am. Chem. Soc. 106, 3613–3623.
25 Macquaire, F., Baleux, F., Giaccobi, E., Huynh-Dinh, T., Neuman, J.-M. and Sanson, A. (1992) Biochemistry 31, 2576–2582.
26 Kunitake, T., Okahata, Y., Ando, R., Shinkai, S. and Hirakawa, S. (1980) J. Am. Chem. Soc. 102, 7877–7881.
27 Fendler, J.-H. and Fendler, E.J. (eds.) (1975) Catalysis in Micellar and Macromolecular Systems, Academic Press, New York.
28 Reynolds, J.A, Tanford, C. and Stone, W.L. (1977) Proc. Natl. Acad. Sci. USA 74, 3796–3799.
29 Smith, R. and Tanford, C. (1972) J. Mol. Biol. 67, 75–83.
30 Rosevear, F.B. (1954) J. Am. Oil Chem. Soc. 31, 629–639.
31 Okahata, Y., Ando, R. and Kunitake, T. (1981) Ber. Bunsenges. Phys. Chem. 85, 789–798.
32 Van Dijck, P.W.K., De Kruijff, B., Van Deenen, L.L.M., De Gier, J. and Demel, R.A. (1976) Biochim. Biophys. Acta 455, 576–587.
33 Shimizu, T., Mori, M. and Hato, M. (1990) J. Chem. Soc. Chem. Commun., 183–185.
34 Bovey, F.A. and Hood, F.P. (1967) Biopolymers 5, 325–326.
35 Yager, P., Sheridean, J.P. and Peticolas, W.L. (1982) Biochim. Biophys. Acta 693, 485–491.
36 Nakashima, N., Asakuma, S. and Kunitake, T. (1985) J. Am. Chem. Soc. 107, 509–510.
37 Yager, P., Schoen, P.E., Davies, C., Price, R. and Singh, A. (1985) Biophys. J. 48, 899–906.
38 Georger, J.H., Singh, A., Price, R.R. Schnur, J.M., Yager, P. and Schoen, P.E. (1987) J. Am. Chem. Soc. 109, 6169–6175.
39 Lee, R.E., Worthington, C.R. and Glew, R.H. (1973) Arch. Biochem. Biophys. 159, 259–266.